S. A. Veress
R. S. Tiwari
University of Washington
Seattle, WA 98195

Fixed-Frame Multiple-Camera System for Close-Range Photogrammetry

The close-range photogrammetric laboratory is self-calibrating and provides fast and accurate three-dimensional measurements.

(*Abstract on next page.*)

Introduction

Since 1966 the University of Washington has been engaged in the use of photogrammetry in various fields of biomedical science. The main purpose and thus the conclusion of this use was to prove that photogrammetry can advantageously be used in bioengineering and in medicine[11]. This advantage in general comes from the fact that photogrammetry is a non-destructive measuring science. Thus it is capable of performing research and diagnostic tasks.

During this period, however, no extensive research was possible because the research was sponsored by only minimal local funds. In most cases the conclusion of the investigation pointed out the possibility and the advantage of the method without entering into the analysis of technical and economical performance.

In August 1974 the National Science Foundation provided a grant to the University of Washington which enabled the University to enter into meaningful biophotogrammetric research with Drs. F. G. Lippert, M.D., and S. A. Veress, D.Sc., as principal investigators. Such a research required the establishment of a close-range photogrammetric laboratory whose design criteria and operating principles will be described in the following sections.

Design Criteria

There are large size differences existing in the specimens in the biomedical field. This size ranges from 2-3 cm to the full size of a human subject of nearly 2 m. Such size differences must be taken into account in the design of a close-range photogrammetric laboratory.

The accuracy requirement of a biomedical subject also varies substantially from 40-50 micrometers to more than one millimeter[6]. This further means that the geometry of the cameras should change according to these requirements. The geometric change in the camera system brings change also in methodology; namely, stereo as well as convergent analytical photogrammetry must be employed according to the accuracy needs of the measurement.

The form of data acquisition in the biomedical field is also subject to variation[8]. In many instances quantitative or numerical data is desirable. In other instances graphical output is required. This graphical output can be computer-generated from numerical data or directly obtained by plotting of "fixed" based stereo photographs.

The biomedical subject may be still or can be in motion[1,9]. Thus the minimum of two cameras is needed for these motion studies. The cycling time of these cameras should be one second or more; if shorter cycling time is required, then the problem must be solved by illumination of strobe lights. This solution has the disadvantage that it must be done in a darkened room with open camera chamber.

Last, but not least, the use of analytical or computational photogrammetry requires a

Photogrammetric Engineering and Remote Sensing,
Vol. 42, No. 9, September 1976, pp. 1195-1210.

control field consisting of several well-defined points in the object space. Such a control field drastically reduces the accessibility of the subject or the mobility of the patient. It is, therefore, necessary that effort should be made for design methodology which would eliminate the control field, which requires having fixed camera stations.

Summarizing these requirements: a system of cameras should be established whereby various camera stations are established with known (calibrated) orientation elements. The depth of field, as well as the photographic distance, should accommodate the size of the

ABSTRACT: *The fixed-frame multiple-camera system is described for measurement in the field of close-range photogrammetry, particularly in the field of bio-medicine. The design criterion is given for specimens ranging from 2-3 centimeters up to 2 meters. The laboratory consists of a geometrical arrangement of three MK-70 metric Hasselblad cameras. The framework provides a reference system and the frame is established from triangular shaped steel tubes pressed into a solid joint.*

The calibration of that system is described along side the methodoloy which is used. The methodology consists of determination of the coordinates of the camera stations by space resection and determination of the orientation elements of each camera station by analytical photogrammetry. These quantities after the calibration are regarded as fixed quantities.

Subject has been determined by analytical space intersection which is the computation process in itself for the individual specimen. It has been found that the calibration using the negatives in transformation for reseau *cameras ranges from three to six micrometers in the photo-coordinate system. The accuracy of the camera station coordinates determined by space resection is around 40-60 micrometers and the orientation elements also have been determined. The result of the space intersection from these fixed cameras is that the standard error is found to range from 0.8 of a millimeter to 0.1 of a millimeter, depending upon the camera configuration in general.*

These standard errors are regarded as satisfactory for most close-range photogrammetry. It has been found that the close-range photogrammetric laboratory is capable of providing fast and accurate three-dimensional measurement, particularly applied to the field of orthopaedics, and it was found that the laboratory has been utilized by various departments at the University of Washington, particularly the Department of Orthopaedics, Department of Orthodontics, and the School of Dentistry, besides the Department of Civil Engineering.

human body as maximum subject size. In order to achieve good accuracy, convergent analytical photogrammetry should also be used with the minimum of three cameras. For stereoscopic observation stereophotographs should be employed. These photographs should have "fixed" bases of various length for accommodation of the changing dimension of specimens. The motion studies would need a relatively short cycling time such as one second and an illumination system, strobes, which would permit 1/4 cycling time with multiple exposure.

REFERENCE SYSTEM

In order to eliminate the control points, and accommodate the "fixed" base stereo or convergent photography, a reference system has been established on which the cameras are mounted. The reference system provides a fixed three-dimensional coordinate system in which the camera positions are determined in the form of coordinates of camera stations (frontal nodal points of the objective) and orientation matrices.

The reference system is manufactured of steel tubes pressed into solid joints combined in a triangular shaped geometry. The reference system is exhibited in Figure 1-A, 1-B, and 1-C.

The steel tubes are 2×3 inches pressed into aluminum joints and mounted into the concrete floor and ceiling. The building in which the laboratory is located vibrates at 10 cycles per minute which required specially selected rubber clamping mounts, thus creating a rigid system.

In Figure 1-A, the locations of cameras are numbered 1-7 and are illustrated by squares. The number 1, number 2 and number 3 camera stations are convergent stations. The number 1 and number 2 have a base of 2.00 meters and the convergency angle (angle between the camera axis and the base) is 67°. The third camera station has a height of 2.10 meters and the angle between the vertical direction and the camera axis is 52°.

The number 4 and number 5 camera stations are the "fixed" base stations having the base of 610 mm and their camera axes are parallel. These two stations can also be combined with the number 3 station to obtain a special form of analytical photogrammetry.

The number 6 and number 7 stations are for stereophotographs with a 180 mm base line for the object size of about 30-50 mm to 300 mm.

Figure 1-B indicates the geometry showing the camera axes. The rays of the convergent camera positions number 1 and number 2 intercept each other at the point of interest by 40°-60° depending on the photographic distance of the point which has the range from 1.5 to 2.5 m. The average angle between the rays of number 3 camera and number 1 and number 2 is about 55°, thus providing a nearly ideal geometry.

Figure 1-C is a photograph of the reference system.

The camera system employed in the laboratory consists of three 70 mm Hasselblad (MK-70) cameras distinguished by their numbers 1146, 1148, and 1149 (referred subsequently as 146, 148, and 149). Two of the cameras, 146 and 148, are a factory matched pair, having exactly the same calibrated focal length of 61.24 mm at infinity. Cameras 146 and 148 have been planned to be used for stereo-photogrammetric purposes while the camera 149, along with 146 and 148, shall be used for convergent analytical photogrammetric determinations. Each camera has a precisely calibrated *reseau* plate with 25 crosses in the form of a 1×1 cam grid intersection for precise measurements and calibration.

The cameras have a one-second recycling time up to *f*/45 *f*-stop and are factory calibrated to the photographic distances of ∞, 15, 5 and 1.6 m.

Considering Figure 1-A as the back of the reference frame, left locations number 1, 4 and 6 are meant exclusively for camera 146 and right locations number 2, 5 and 7 for camera 148. Camera 149 shall always be positioned at location number 3. Each camera base has a precisely machined plate rigidly fixed to it, so that when the cameras are removed and replaced on the respective platforms, they recapture their orientation to within 50 microns.

Methodology

The methods to be used in the laboratory should be selected so that they serve dual purposes, namely, diagnostic and research. As a consequence the return time, that is the time

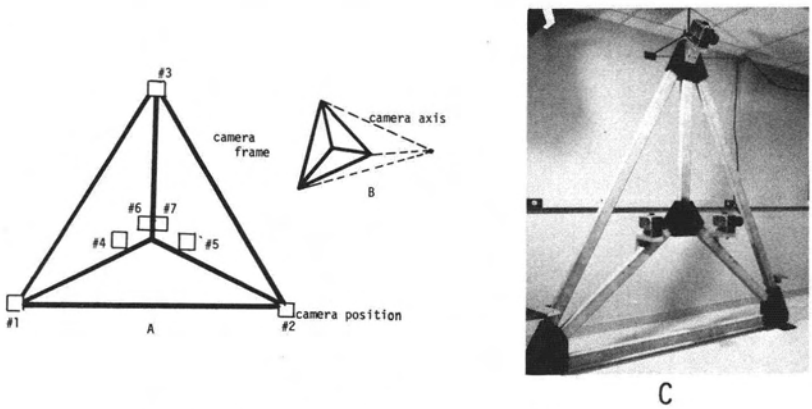

Fig. 1. Camera locations on the reference frame.

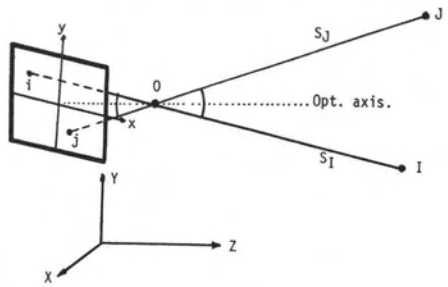

FIG. 2. Coordinate system for space resection.

elapsed from data acquisition to data reduction, should not be more than 24-48 hours. This can be accomplished only if one uses fixed orientation elements either for stereo or convergent photography.

In stereo-photogrammetry the fixed orientation elements eliminate the process of absolute and relative orientation by having a plotter with the same fixed orientation elements. Thus a direct map production is possible. In analytical photogrammetry the fixed orientation elements mean that the orientation matrices of the camera station and their space coordinates are fixed input values. Only the location of new points must be determined by space intersection.

Consequently the methodology can be divided into two major parts; one is the calibration and the other, production of space coordinates of points of interest. The calibration includes the space resection and determination of camera orientation[3,9]. The actual photogrammetric production consists of space intersection. (See Figure 3.)

A number of space resection methods are known in literature[10]. One of the most popular is based on the collinearity equations. In this method, the coordinates of the camera station and the orientation matrix are solved simultaneously. In order to test the sensitivity of various types of resections, a mathematical model has been computed and used for testing. The space resection described in the following and illustrated in Figure 2 gave the best results.

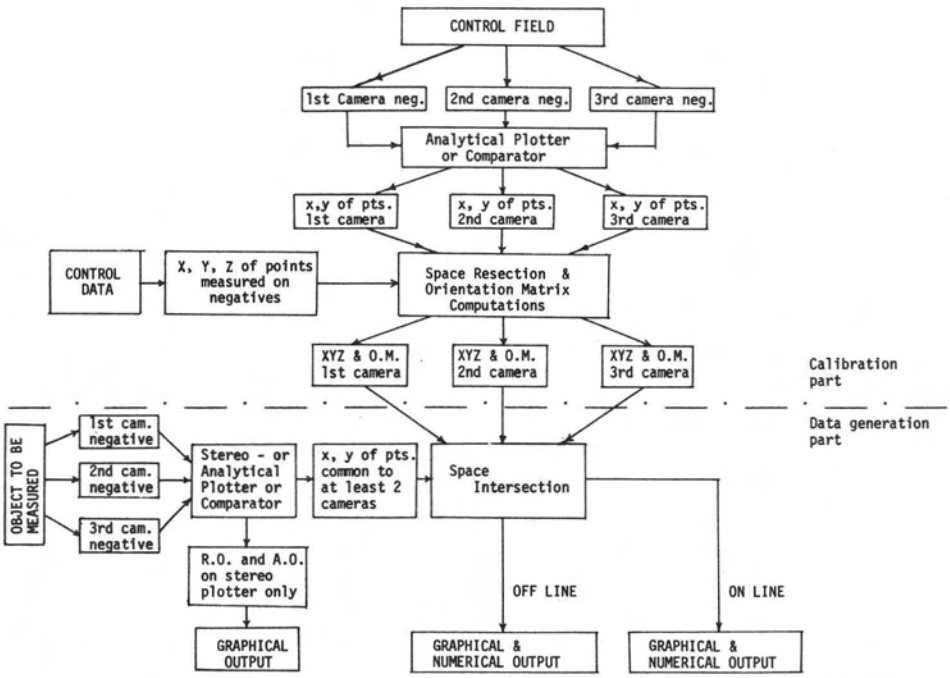

FIG. 3. Sequence of data processing for a three camera analytical photogrammetric system.

This was attributed to the sensitivity of the cosine function of the angles toward the control point on which the method is based.

The purpose of the space resection is to determine space coordinates of the frontal nodal point of the camera which will be called the perspective center. The coordinates of *0* perspective center are X, Y, and Z.

Approximate coordinates are: X_o, Y_o, and Z_o estimated. The principle of the computation according to Figure 2 is—

$$\cos(ij) = \cos(IJ) \tag{1}$$

where

$$\cos(IJ) = \frac{x_i x_j + y_i y_j + f^2}{S_i \cdot S_j}$$

$$S_i = \sqrt{x_i^2 + y_i^2 + f^2} \qquad S_j = \sqrt{x_j^2 + y_j^2 + f^2}$$

The $\cos(IJ)$ cannot be computed because the X, Y, Z coordinates are unknown. The approximate value computed of the cosine of the same angle in the object space is—

$$\cos(IJ)_0 = \frac{(X_o - X_I)(X_o - X_J) + (Y_o - Y_I)(Y_o - Y_J) + (Z_o - Z_I)(Z_o - Z_J)}{S_I \cdot S_J}$$

where

$$S_I = \sqrt{(X_o - X_I)^2 + (Y_o - Y_I)^2 + (Z_o - Z_I)^2}$$

$$S_J = \sqrt{(X_o - X_J)^2 + (Y_o - Y_J)^2 + (Z_o - Z_J)^2}$$

Equation 1 using approximate values modifies to

$$\cos(IJ)_o + \frac{\partial \cos(IJ)}{\partial X_o}\Delta X \frac{\partial \cos(IJ)}{\partial Y_o}\Delta Y \frac{\partial \cos(IJ)}{\partial Z_o}\Delta Z = \cos(ij)$$

Then the general observation equation may be shown as

$$\begin{array}{cccccc} a_{ij}\Delta X + b_{ij}\Delta Y + c_{ij}\Delta Z - \cos(ij) - \cos(IJ)_o = v_{ij} \\ \cdot & \cdot & \cdot & \cdot & \cdot & \cdot \\ \cdot & \cdot & \cdot & \cdot & \cdot & \cdot \\ \cdot & \cdot & \cdot & \cdot & \cdot & \cdot \end{array} \tag{2}$$

or

$$\boldsymbol{AX} - \boldsymbol{L} = \boldsymbol{V}$$

where the partial derivatives are—

$$\frac{\partial \cos(IJ)}{\partial X} = \frac{(X_o - X_I) + (X_o - X_J)}{S_I \cdot S_J}$$

$$- \left[\frac{(X_o - X_I)(X_o - X_J) + (Y_o - Y_I)(Y_o - Y_J) + (Z_o - Z_I)(Z_o - Z_J)}{S_I \cdot S_J} \right] \left[\frac{(X_o - X_J)}{S_J^2} + \frac{(X_o - X_I)}{S_I^2} \right]$$

which simplifies to

$$T_{IJ} = \frac{\frac{S_I \cos(ij)}{S_J}}{S_I \cdot S_J}$$

Thus

$$a_{ij} = (X_o - X_I)\, T_{JI} + (X_o - X_J)\, T_{IJ}$$
$$b_{ij} = (Y_o - Y_I)\, T_{JI} + (Y_o - Y_J)\, T_{IJ}$$
$$c_{ij} = (Z_o - Z_I)\, T_{JI} + (Z_o - Z_J)\, T_{IJ}$$

If there are n points in the object space, the number of angle combination is $n(n-1)/2$. For three points there is a unique solution. For four points there are six angle combinations. Thus the number of equations are six in Equation 2.

It must be noted that from a theoretical point of view the least-squares adjustment as it is presented here is incorrect because the corrections (v's) are rendered to the differences of the cosines rather than to the observed quantities of plate coordinates x and y. Consequently the purpose of the least-square adjustment here is to obtain the best fit between image and object space.

Using the proper number of angle combinations, compute the

$$\boldsymbol{AX} - \boldsymbol{L} = \boldsymbol{V}$$

matrix. Then the normal equation is

$$\boldsymbol{A}^T\boldsymbol{AX} - \boldsymbol{A}^T\boldsymbol{L} = 0.$$

Solve for

$$\boldsymbol{X} = (\boldsymbol{A}^T\boldsymbol{A})^{-1}\,\boldsymbol{A}^T\boldsymbol{L}.$$

The coordinates of the perspective center 0 are

$$X' = X_o + \Delta X$$
$$Y' = Y_o + \Delta Y$$
$$Z' = Z_o + \Delta Z \qquad (3)$$

These are the inputs for second iteration. The iteration continues until

$$\Delta X = \Delta Y = \Delta Z \rightarrow 0.$$

The next and last step in the calibration process is to determine the orientation matrix of each camera station. The orientation matrix will then be handled as calibrated or "fixed" quantity for each photograph taken from that station.

The basic principle of the computation is the mathematical comparison of vector $(\vec{S}_a)$ coming from the perspective center of the lens to the image point to the vector $(\vec{S}_A)$ between the perspective center and the object point (A).

Let us consider there are three points given A, B, and C. The ground coordinates are X_A, Y_A, Z_A, X_B, Y_B, Z_B, and X_C, Y_C, Z_C. The photo coordinates are x_a, y_a, x_b, y_b, x_c, and f. Further the station coordinates are X, Y, and Z.

The vector of $a0$ in the picture space defined as:

$$\vec{\boldsymbol{S}}_a = \begin{bmatrix} \dfrac{-x_a}{\sqrt{x_a^2 + y_a^2 + f^2}} \\ \dfrac{-y_a}{\sqrt{x_a^2 + y_a^2 + f^2}} \\ \dfrac{f_a}{\sqrt{x_a^2 + y_a^2 + f^2}} \end{bmatrix} = \begin{bmatrix} \cos xaO \\ \cos yaO \\ \cos zaO \end{bmatrix}$$

Similarly in the object space:

$$\vec{S}_A = \begin{bmatrix} \frac{X_O - X_A}{OA} \\ \frac{Y_O - Y_A}{OA} \\ \frac{Z_O - Z_A}{OA} \end{bmatrix} = \begin{bmatrix} \cos XAO \\ \cos YAO \\ \cos ZAO \end{bmatrix}$$

where

$$AO = \sqrt{(X_O - X_A)^2 + (Y_O - Y_A)^2 + (Z_O - Z_A)^2}$$

The direction cosines formed between the coordinate axes and AO line, etc. If $\boldsymbol{M}$ is formed for negatives, the orientation matrix, the relation between the two vectors is

$$\boldsymbol{M} \cdot \vec{S}_A = \vec{S}_a$$

or in detail

$$\begin{bmatrix} m_{11}\ m_{12}\ m_{13} \\ m_{21}\ m_{22}\ m_{23} \\ m_{31}\ m_{32}\ m_{33} \end{bmatrix} \begin{bmatrix} \cos XAO \\ \cos YAO \\ \cos ZAO \end{bmatrix} = \begin{bmatrix} \cos xaO \\ \cos yaO \\ \cos zaO \end{bmatrix}$$

Because the $\boldsymbol{M}$ has nine terms in it the minimum of three points are required to solve for $\boldsymbol{M}$. That is

$$\boldsymbol{M}\,(\vec{S}_A\ \vec{S}_B\ \vec{S}_C) = \vec{S}_a\ \vec{S}_b\ \vec{S}_c$$

from here

$$\boldsymbol{M} = (\vec{S}_a\ \vec{S}_b\ \vec{S}_c)\ \ (\vec{S}_A\ \vec{S}_B\ \vec{S}_C)^{-1} \tag{4}$$

This equation may be solved in three separate computations if the above equations are expanded. The least-squares adjustment must be used if more than three points are given, as follows:

$$\begin{aligned} &\cos XAO\ m_{11} + \cos YAO\ m_{12} + \cos ZAO\ m_{13} - \cos xaO = v_1 \\ &\cos XBO\ m_{11} + \cos YBO\ m_{12} + \cos ZBO\ m_{13} - \cos xbO = v_2 \\ &\quad\vdots \end{aligned}$$

or in general form:

$$\boldsymbol{AX} - \boldsymbol{L} = \boldsymbol{V}$$

where

$$\boldsymbol{X} = \begin{bmatrix} m_{11} \\ m_{12} \\ m_{13} \end{bmatrix}$$

the rest of the matrices are easily identifiable and the unknowns solved in the usual manner.

It should be noted that the $\boldsymbol{M}$ matrix is an orthogonal matrix, composed of three rotational angles and a scale factor. In the above solution the orthogonality of $\boldsymbol{M}$ matrix is destroyed and transferred into an affine matrix with three scale factors. This provides a better fit particularly for close-range photogrammetry where the accuracy of the control field and the

camera station are more critical than in conventional photogrammetry and neither of these parameters could be considered as errorless.

The actual photogrammetric production consists of determining spatial position points in the object space by space intersection. The advantage of separating this phase of computation from the previous ones is that each point is computed individually. Thus any mistaken or undesirable point can be rejected without having an effect on the rest of the points which is the case in simultaneous adjustment. Further, it may be regarded as an advantage that the largest size of the equations to be solved simultaneously are three. Thus any small-sized computer can be utilized.

The space intersection is not an iterative process because the approximate coordinates of object points should be computed first in order to enter into a least-squares adjustment with nearly correct values.

The following mathematical notation may be used to express the situation:

$$\begin{aligned} X_p &= X_o - \Delta X \\ Y_p &= Y_o - \Delta Y \\ Z_p &= Z_o - \Delta Z \end{aligned} \tag{5}$$

where X_p, Y_p, and Z_p are the point coordinates in the object space; X_o, Y_o, and Z_o represent the approximate coordinates; and ΔX, ΔY, and ΔZ are the differential coordinates to be determined by the least-squares adjusted space intersection.

The given quantities are X_{O_1}, Y_{O_1}, Z_{O_1}, X_{O_2}, Y_{O_2}, Z_{O_2} coordinates of camera station O_1 and O_2 and the $\boldsymbol{M}'$ and $\boldsymbol{M}''$ orientation matrices.

The equation of the line from O_1 to P point is

$$\frac{X_o - X_{O_1}}{\cos XO_1P} = \frac{Y_o - Y_{O_1}}{\cos YO_1P} = \frac{Z_{O_1} - Z_o}{\cos ZO_1P}$$

Similarly for line O_2P

$$\frac{X_o - X_{O_2}}{\cos XO_2P} = \frac{Y_o - Y_{O_2}}{\cos YO_2P} = \frac{Z_{O_2} - Z_o}{\cos ZO_2P}$$

From these equations the approximate coordinates can be solved the following way:

$$Z_o = \left[X_{O_2} - X_{O_1} - Z_{O_1} \frac{\cos XO_1P}{\cos ZO_1P} + Z_{O_2} \frac{\cos XO_2P}{\cos ZO_2P} \right] \left[\frac{1}{\dfrac{\cos XO_2P}{\cos ZO_2P} - \dfrac{\cos XO_1P}{\cos ZO_2P}} \right]$$

which further yields

$$X_o = (Z_{O_1} - Z_o) \frac{\cos XO_1P}{\cos ZO_1P} + X_{O_1}$$

and

$$Y_o = (Z_{O_1} - Z_o) \frac{\cos YO_1P}{\cos ZO_1P} + Y_{O_1} \tag{6}$$

The required direction cosines computed from the picture coordinates and modified by the orientation matrix.

$$\cos XO_1P = m'_{11} \frac{x_1}{O_{1P}} + m'_{12} \frac{y_1}{O_{1P}} + m'_{13} \frac{f}{O_{1P}}$$

. . . .

. . . .

. . . .

and

$$\cos XO_2P = m''_{11}\frac{x_2}{O_{2p}} + m''_{12}\frac{y_2}{O_{2p}} + m''_{13}\frac{f}{O_{2p}}$$

$$\vdots \qquad \vdots \qquad \vdots \qquad \vdots$$

where

$$O_{1p} = \sqrt{x^2{}_1 + y^2{}_1 + f^2} \text{ and } O_{2p} = \sqrt{x^2{}_2 + y^2{}_2 + f^2}$$

It may be noted that there are a number of other solutions to obtain approximate coordinates; some of these solutions are particularly simple if the coordinate system is chosen so that its x axis is parallel to the camera base line. The above solution was selected because of the more general nature, being independent from the orientation of spatial coordinate system.

Having the approximate coordinates, the space intersection can be computed. Consider three camera stations for which the given quantities are $\boldsymbol{M}'$ and $\boldsymbol{M}''$ and $\boldsymbol{M}'''$ orientation matrices and the coordinates of the camera stations are $X_{O_1}, X_{O_2}, X_{O_3}, Y_{O_1}, Y_{O_2}, Y_{O_3}, Z_{O_1}, Z_{O_2}, Z_{O_3}$. Measured are the point coordinates $x'_i, y'_i, f'_i; x''_i, y''_i, f''_i;$ and x'''_i, y'''_i, f'''_i, for the three negatives.

The collinearity equations:

$$x' = f' \frac{\boldsymbol{M}'_1 X'}{\boldsymbol{M}'_3 X'} \qquad y' = f' \frac{\boldsymbol{M}'_2 X'}{\boldsymbol{M}'_3 X'}$$

$$x'' = f'' \frac{\boldsymbol{M}''_1 X''}{\boldsymbol{M}''_3 X''} \qquad y'' = f'' \frac{\boldsymbol{M}''_2 X''}{\boldsymbol{M}''_3 X''}$$

$$x''' = f''' \frac{\boldsymbol{M}''' X'''}{\boldsymbol{M}'''_3 X'''} \qquad Y''' = f''' \frac{\boldsymbol{M}'''_2 X'''}{\boldsymbol{M}'''_3 X'''} \tag{7}$$

The observation equations from these formulas are in general and detailed form:

$$\boldsymbol{V} = \boldsymbol{A}\boldsymbol{X} - \boldsymbol{L}$$

$$v_{x'} = \frac{\partial F'_1}{\partial X}\Delta X_i + \frac{\partial F'_1}{\partial Y}\Delta Y_i + \frac{\partial F'_1}{\partial Z}\Delta Z - [x' - F'_1(X_{o1}\, Y_{o1}\, Z_o)]$$

$$v_{x''} = \frac{\partial F''_1}{\partial X}\Delta X_i + \frac{\partial F''_1}{\partial Y}\Delta Y_i + \frac{\partial F''_1}{\partial Z}\Delta Z - [x'' - F''_1(X_{o1}\, Y_{o1}\, Z_o)]$$

$$\vdots \qquad \vdots \qquad \vdots \qquad \vdots$$

$$v_{y'} = \frac{\partial F'_2}{\partial X}\Delta X_i + \frac{\partial F'_2}{\partial Y}\Delta Y_i + \frac{\partial F'_2}{\partial Z}\Delta Z - [y' - F'_2(X_{o1}\, Y_{o1}\, Z_o)]$$

where the corresponding matrices are easily identifiable.

Normal equations are—

$$\boldsymbol{A}^{\mathrm{T}}\boldsymbol{A}\boldsymbol{X} - \boldsymbol{A}^{\mathrm{T}}\boldsymbol{L} = \mathrm{O}$$

and

$$\boldsymbol{X} = (\boldsymbol{A}^{\mathrm{T}}\boldsymbol{A})^{-1}\boldsymbol{A}^{\mathrm{T}}\boldsymbol{L}$$

The standard error of unit weight and the standard error of the most probable values of the coordinates are—

$$\sigma_o = \sqrt{\frac{\boldsymbol{V}^{\mathrm{T}}\boldsymbol{V}}{n-u}} \qquad \sigma_x = \sigma_o\sqrt{\boldsymbol{Q}_{xx}}$$

where n is the number of observations, u the number of unknowns, and Q_{xx} is the diagonal of the inverse of the coefficient matrix of the normal equation.

The sequence of steps involved in the computation is shown in Figure 3, where the calibration and the data generating parts are separated by a dotted line.

The Control Field

A three-dimensional control field has been established in the object space for the calibration and testing of the reference system. The control field consists of four piano wires which are suspended as plumb lines with heavy plumb bobs in oil bath at one end and fixed to the ceiling by hooks at the other. The wires along with hooks can be taken from the ceiling and stored for use in future calibrations.

Each wire has four steel balls, 2 mm in diameter, fixed so that they are well distributed in the negatives when photographed. The balls are numbered serially from 1 to 16 to serve as the target points. The two outer wires are located at 2 meters from the reference frame while the two middle wires are at 1.70 meters, thus proving a variation in the third dimension. The lateral spacing of the wires is such that at least three of these appear on each negative obtained from normal camera positions (3 and 5 in Figure 1-A). The negatives from other camera locations (except 6 and 7) contain all the four wires so that enough common points are available to test the system design for the photogrammetric production of points. Figure 4-A to 4-E shows the control field coverage on negatives from various camera locations.

Precise theodolite surveys were carried out to determine the object space coordinates of the control points. Two Wild T2 theodolites were used to measure the horizontal and vertical angles to the target points from the end of a base line, which was accurately measured by a steel tape lying flat on the floor. A total of six sets of angular measurements were obtained. It was found that the increase in number of angle measurements would not improve the results due to the larger influence of eccentricity in the instrumental set up.

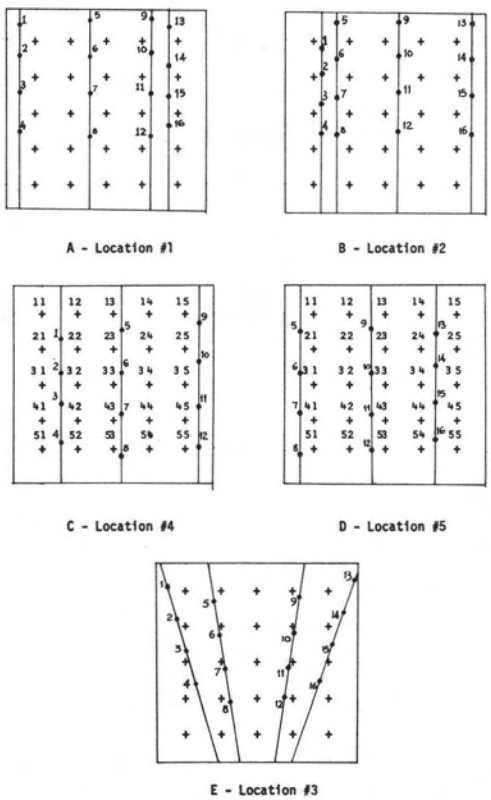

FIG. 4. Control field coverage of negatives from various locations.

A number of photographs of the control field were taken during the theodolite measurements, from the various camera locations. The photography was repeated several times by removing the cameras from their positions and replacing them so as to find out the changes in orientation elements.

Data Reduction

Selected negatives, obtained after processing, were observed monocularly on the analytical plotter AP/C in the usual manner. On each negative the measurements of x, y coordinates of 25 *reseau* crosses were first carried out and thereafter the control points were measured. For each reference the *reseau* crosses are designated by numbers using the matrix notation as shown in Figure 4-C, along with the camera numbers, negative code, and data of photography.

Data were processed on the CDC 6400 computer at the University of Washington. A number of programs in Fortran IV have been developed for the various stages of computations. Details of these along with a discussion of the results obtained are given in the following.

The control survey data were reduced to discover the object space coordinates of the target points with respect to arbitrarily chosen coordinates of one of the theodolite stations as origin. The coordinate system, as shown in Figure 2, was chosen so that X-axis is along the base line and Y-axis is in the vertical direction.

The computed coordinates of the target points from the various sets were found to be consistent to within 100 micrometers.

The observed negative coordinates must be reduced in the image coordinate system before they can be used as data for the calibration computations. This was carried out in three steps:

(i) Reduction of observed coordinates to negative center: For this the coordinates of the center of the negative were found by taking the mean of the observed coordinates of four symmetrically located *reseau* crosses. More numbers of *reseau* crosses at symmetrical locations may be used for this purpose but it was found that even by using all the 25 crosses there was no significant difference in the coordinates. It was decided to use only four points subsequently to keep in conformity with the general photogrammetric systems where four fiducial marks are employed for this purpose. All observed coordinates are then reduced with respect to the negative center.

(ii) Transformation of the negative coordinates to supplied calibration data: The calibration data supplied by the manufacturers, for each camera, is in the form of deviations of the *reseau* crosses from their nominal positions with respect to one corner point as origin. This data was first reduced in the form of coordinates with respect to central *reseau* cross in the same coordinate system as used in the negative measurement, and then was used for transformation of the observed coordinates.

Theoretically, transformations can be carried out in a number of ways. The two most common methods in use are (i) the similarity (Helmert's) transformation which involves two translations and an orthogonal rotation without any scale change which is regarded constant along X and Y directions; and (ii) the affine transformation which takes into account errors in perpendicularity between the x and y comparator coordinate axes and possible linear distortion along X and Y directions due to emulsion deformation, lens distortion, etc. The mathematical equations for these transformations are well known. For similarity transformation two points and for affine three points, in both measured and transformed coordinate systems, are required for unique solution. If more points are available, a least-squares solution may be carried out.

In the present case, since there are 25 *reseau* crosses with known calibration data, any number of these may be used for the transformation. In actual use, however, all the 25 crosses may not be available for measurement because some of these might be unidentifiable in the background of the objects being photographed. In such cases a decision, concerning how many points and at which locations these should be chosen for transformation, has to be made.

As a side investigation, therefore, both similarity and affine transformations were carried out using 4, 8, 15, and 25 points at symmetrical as well as random locations using the same data in each case. The standard errors in x and y in each case were obtained as given in Table 1. The variation in standard errors for the different cases was too small to be of any practical

TABLE 1. RESULTS OF THE CONFORMAL AND AFFINE TRANSFORMATIONS.

Negative No.	No. of Points Used	Standard Error in Micrometers							
		Conformal				Affine			
		Symmetrical		Random		Symmetrical		Random	
		x	y	x	y	x	y	x	y
146-N10R	4	4.08	3.50	6.08	3.19	3.66	3.39	6.13	3.79
	8	3.97	3.34	3.81	3.85	3.64	3.01	3.72	3.45
	15	4.18	3.21	3.83	3.42	3.79	3.01	3.59	3.04
	25	3.85	3.32	—	—	3.52	2.93	—	—
148-N10R	4	3.45	5.02	3.72	3.81	3.54	4.69	3.52	8.41
	8	3.35	4.20	3.48	3.51	3.32	3.84	3.19	3.70
	15	3.17	3.82	3.30	3.77	3.03	3.44	3.21	3.35
	25	3.29	3.58	—	—	3.00	3.32	—	—
149-N10R	4	4.72	4.92	4.51	7.33	4.24	4.51	4.05	4.43
	8	3.94	4.51	4.54	5.27	3.44	4.03	3.89	4.87
	15	3.83	4.25	4.03	4.09	3.31	3.80	3.09	4.02
	25	3.69	4.27	—	—	3.08	3.76	—	—

significance. The standard errors, both in x and y, in case of affine transformation, were in general smaller than those by conformal transformation and in most cases the errors were reduced when the number of transformation points was increased to 25. The distribution of points did not show anything significant enough to draw any conclusion, although symmetrical location is generally preferred. On the basis of this study, affine transformation with eight or more available points, preferably in symmetrical location, were used for subsequent data reductions.

(iii) Reduction of transformed coordinates to auto collimation point: The image coordinates obtained after transformation are with respect to the center of the negative and not the principal point. The coordinates must be corrected before these are used for space resection and other computations, using the calibration data for this purpose.

The reduced image coordinates of the targets, as obtained after transformation for different negatives from the same camera location, were compared to find out the precision obtainable from the system when the cameras are removed and replaced to their positions. The standard deviation of coordinates for two negatives taken on different dates, after the cameras were removed and replaced, were found for each camera location.

The maximum deviation in x and y coordinates for the various locations was found to be less than 25 micrometers. In almost all cases the signs of deviation were either positive or negative indicating a systematic error in play. Though the actual cause of this error has not yet been conclusively found, it presumably is caused by the rotation of the frame due to either the building vibrations or disturbances at the time of removing or replacing the cameras in position. This must be substantiated by further measurements.

SPACE RESECTION AND INTERSECTION OF POINTS

Based on previously discussed equations, computations were done for space resection of locations number 1 to 5 using the reduced negative data. In all the computations four points were used and a least-squares iterative solution was carried out. Computations for each camera location were repeated by changing the set of four points so as to have a different geometry for the solution, for the same negative. The solution in each case converged after four iterations.

The coordinates of the frontal nodal points of the cameras, for the various camera location, were found to agree closely for different negative data. The discrepancies in most cases were found to be less than 1 mm with the average of 0.605 micrometers. These may be attributed to several factors such as geometry of points, control data errors, non-uniform vibrations of the building, quality of negatives, distortions in film, etc. No special efforts were made to correct these error sources at this time.

For each camera location, three sets of four points providing different geometry were selected for the computation. For each of these sets, orientation matrices were determined by using the corresponding space resection data, and these were used for the space intersection coordinates for the different set of points as obtained above. These were then considered as the fixed calibration data for the space intersection computations by using data from various negatives.

The space intersection computations using the above resection data were carried out for two and three camera cases for both normal and convergent negative data. The computed coordinates were compared in a variety of ways and for each case standard deviations of X, Y, and Z determinations were found as given in Table 2.1 to Table 2.3.

Analysis of the Results

The preliminary results shown in Table 2.1 to 2.3 must not be taken as the final accuracy figures achievable by the system since it is still in the process of modification and refinement. A few error sources, as mentioned earlier, were noticed during the establishment and calibration stages of the system but these either could not be corrected during the computations or were deliberately left out of the computations to see their effect on the final results; for example, systematic errors found in camera location number 3 which were located in the clamping pin of the camera. The use of this data explains partly why the results of three camera intersections are either inferior or have only little improvement over those obtained by the two camera intersection in the various tables. The pin has been changed and the new photography has been processed to compute the new calibration data for the location number 3, which shows no systematic errors.

Table 2.1. Space Intersection Results Using Conventional Approach

Number of Cameras Used	Location of Cameras	Number of Points Intersected	Standard Error of Coordinates in mm.		
			σ_X	σ_Y	σ_Z
3	3, 4, 5	8	0.117	0.119	0.298
3	1, 2, 3	10	0.197	0.225	0.329
2	4, 5	8	0.145	0.169	0.853
2	1, 2	10	0.249	0.268	1.138

Table 2.2. Space Intersection Results Using Fixed Orientation Data Standard Errors of Coordinates of New Points Computed With Respect to Ground Control Data.

Number of Cameras Used	Location of Cameras	Number of Points Intersected	Standard Error of Coordinates in mm.		
			σ_X	σ_Y	σ_Z
3	3, 4, 5	8	0.692	0.248	0.867
3	1, 2, 3	10	0.286	0.238	0.309
2	4, 5	8	0.293	0.141	0.812
2	1, 2	10	0.343	0.193	1.025

Table 2.3. Space Intersection Results Using Fixed Orientation Data: Standard Errors of Coordinates of New Points Computed With Respect to the Coordinates Generated by One of the Negatives.

Number of Cameras Used	Location of Cameras	Number of Points Intersected	Standard Error of Coordinates in mm.		
			σ_X	σ_Y	σ_Z
3	3, 4, 5	8	0.668	0.272	1.129
3	1, 2, 3	10	0.208	0.163	0.259
2	4, 5	8	0.249	0.173	0.558
2	1, 2	10	0.187	0.190	0.287

From the other error sources left out of computations, the more important ones which are mainly responsible for residual errors in coordinate determination (particularly the Z coordinates) are—

(1) *Control data determination.* For the calibration of the close-range system as described herein, a very precise determination of object space control points is of utmost importance. This accuracy requirement often poses a geodetic problem and in many cases is not quite met, presenting a serious limitation to calibration work[4,7]. An alternative in such cases is to carry out a simultaneous adjustment of all the data, including the control data, by treating these as observed quantities rather than fixed. Though this involves a significant increase in the computational work, it is worth carrying out for better accuracy[3,4].

(2) *Principal distance determination.* The calibration data supplied by the manufacturer give the focal length or principal distance of the cameras with a standard error of $\pm$ 10 μm. For close-range work, however, the principal distance must be accurately known for the particular photographic distance which otherwise would give rise to an affine deformation affecting the X, Y, and Z coordinates. The residual principal distance errors give rise to errors in X, Y, and Z coordinate determinations according to the model deformation equations given by Veress[12] for both the normal and the convergent case. As an example, if we consider only the normal case where for the base cameras.

$$\omega' \simeq \phi' \simeq \kappa' \simeq \omega'' \simeq \kappa'' \simeq 0$$

the X, Y, Z coordinate errors due to the residual f-errors for a two-camera system can be obtained as:

$$\partial X_2 = \frac{X}{Z}\ \frac{(x-b_1)}{b_1}\ (df' - df'')$$

$$\partial Y_2 = \frac{Y}{Zb_1}\left(\frac{x+b_1}{2}\right) df' - \frac{Y}{Zb_1}\left(\frac{x-b_1}{2}\right) df''$$

$$\partial Z_2 = \frac{1}{b_1}\ [x df' - (x-b_1)\, df'']$$

If, however, the third camera is considered along with one of the base cameras, then since $\omega''' = 39°$, $\phi''' = 0$, and $\kappa''' = 0$ for the third camera, and the base = b_2, the errors in coordinates will be

$$\partial X_3 = \frac{X}{Z}\ \frac{(x-b_2)}{b_2}\ (df' - \cos\omega'''\, df''')$$

$$\partial Y_3 = \frac{Y}{Zb_2}\left(x + \frac{b_2}{2}\right) df' - \left[\frac{Y}{Zb_2}\left(x - \frac{b_2}{2}\right)\cos\omega''' - \frac{1}{2}\sin\omega'''\right]$$

$$\partial Z_3 = \frac{1}{b_2}\left[x df' - (x-b_2)\cos\omega'''\, df'''\right]$$

These equations may be simplified by assuming the residual f-errors for the three cameras to be the same. This is justified, particularly in the present case, since all the cameras are factory calibrated and matched. Then,

$$\partial X_2 = 0 \qquad \partial Y_2 = \frac{Y}{Z}\ df \qquad \partial Z_2 = df$$

and

$$\partial X_3 = \frac{X}{Z}\ \frac{(x-b_2)}{b_2}\ (1-\cos\omega''')\, df$$

$$\partial Y_3 = \frac{Y}{Zb_2}\left[\left(x + \frac{b_2}{2}\right) - \left(x - \frac{b_2}{2}\right)\cos\omega'''\right] df + \frac{\sin\omega'''}{2}\ df$$

$$\partial Z_3 = \frac{1}{b_2}\left[\, x - (x - b_2)\cos\omega''' \,\right] df$$

Assuming $df = 0.005$ mm, $b_1 = 0.6$ meter, and $b_2 = 1$ meter, as in the present case, the X, Y, and Z coordinate errors for any point having coordinates as (100, 100, 100) for the two cases are—

(i) Using the two base cameras

$$\partial X_2 = 0 \qquad \partial Y_2 = 0.005 \text{ mm.} \qquad \partial Z_2 = 0.005 \text{ mm.}$$

(ii) Using one of the base cameras and the third camera

$$X_3 = 99\,(1 - \cos 39°)\,0.005 \text{ mm} = 0.110 \text{ mm.}$$

$$Y_3 = (100 \cdot 5 - 99.5 \cos 39°) + \frac{\sin 39°}{2} \times 0.005 = 0.115 \text{ mm.}$$

$$Z_3 = (100 - 99 \cos 39°)\,0.005 = 0.115 \text{ mm.}$$

Because of the symmetrical location of the base cameras with respect to the third, the X, Ycoordinate errors get compensated in a three-camera system and do not affect these coordinates, but the Z errors act in the same direction affecting the Z coordinates. Similar computations can be carried out for the convergent case with almost similar results. This effect of the residual f-errors, along with the systematic errors in image coordinates from location number 3, as already mentioned, explains the lower accuracy of the Z-coordinates.

This analysis emphasizes the importance of proper knowledge of interior orientation elements which have a substantially larger influence on close-range works than conventional photogrammetry works, a fact already reported by several authors[3,7].

(3) Variations of the distortion characteristics of cameras: The camera calibration data supplied by the manufacturer include the distortion characteristics of the lens. However, as reported by Kenefick[7] "... analytical calibrations of cameras focused at infinity can not generally be applied directly to close range work since the distortion of a lens varies with focus ... Perhaps of even greater consequence is the variation of distortion within the depth of field for a unique finite distance focus setting." The effect of distortion errors has not been considered significant for the present case and hence no attempt was made to correct the same in the computations.

These discussions of some of the error sources apply directly to the results given in Table 2.1 to 2.3 and it is easier to analyze these in this perspective. Table 2.1 gives the standard errors obtained by employing a purely conventional approach, i.e., computing the space resection data for each negative separately and using the same for the production of new points by intersection. The standard errors of the coordinates were found by comparing the generated coordinate with the control data. This approach gives the best result of the various methods that have been discussed here.

Table 2.2 shows the result of the fixed orientation elements system. The space resection data obtained from one set of negatives were considered fixed and were used in generating new points from other negative data by space intersection. The standard errors in this case, also, were computed with respect to the ground control data. The results in this case, as anticipated, are inferior to those obtained by using the conventional approach.

For further investigation the results of two sets of negatives were compared among themselves rather than with ground control data. Table 2.3 gives the standard errors obtained from this comparison for the 2 and 3 camera cases for both normal and convergent photography. Improvement in accuracies for the two camera cases particularly in X and Z coordinates is significant. A slight improvement for the three-camera convergent case is also noticed but the results deteriorate for the three-camera normal case.

Finally, the systematic errors inherent to the design camera stations were corrected and a new experiment was executed whereby the cameras as well as the control field were removed and reestablished. Photographs were made before and after these changes and the average residual standard errors after space intersection were found to be $\sigma_x = \pm 218\ \mu$m, $\sigma_y = \pm 338\ \mu$m, and $\sigma_z = 911\ \mu$m. These have been regarded as satisfactory for close-range photogrammetry.

Conclusions

A close-range photogrammetric laboratory to provide fast and accurate three dimensional measurements for biomedical purposes has been established. The preliminary results of the calibration of the analytical photogrammetric system of the laboratory shows the feasibility of the planned approach. Though the achievable accuracy can be further improved upon, it is considered good at this initial stage of the establishment.

For practically all applications in the orthopedics field, the accuracy desired in three-dimensional measurements is well under that achievable by the system at present. The system has therefore been made operational for actual practical applications and a few cases have already been taken. Further improvements of the system will be carried out simultaneously with these applications.

At present, experiments show that the photographs and their processing can be done within six hours, data reduction in four to six hours depending upon the number of points to be generated. If additional presentations of data are required in the form of computer graphics, this means that the time requirement further increases. However, it must be pointed out that the system as it is designed and presently being constructed is capable of performing two basic tasks, namely diagnosis and research.

The close-range photogrammetric laboratory at the University of Washington is being used and will be used by the following departments: Department of Orthodontics, Department of Orthopedics, School of Dentistry, and the Department of Civil Engineering which also provides the data measurement and reduction facility. Studies include patellar motions, and facial and scalp measurements. Additional studies are being formulated.

Acknowledgment

The support provided by the National Science Foundation for the work reported in this paper is gratefully acknowledged.

Due credit should be given to Mr. S. A. Feher, currently a graduate student at the University of Washington, for helping in the camera system design and for putting it in operation.

Sincere thanks and appreciation are also due to Aerial Mapping Company of Oregon for donating the Balplex projector to the University of Washington. It greatly increases the productivity and flexibility of production of the laboratory.

References

1. Ayoub, M. A., and M. M. Ayoub, "Stereophotogrammetry in Human Motion Analysis," *Proceedings* of 36th Annual Meeting, A. S. P., 1970.
2. Brown, D. C. *A Solution to the General Problem of Multiple Station Analytical Stereotriangulation*, R.C.A. Data Reduction Technical Report, No. 43, 1958.
3. Brown, D. C. "Analytical Calibration of Close-Range Cameras," A.S.P. Symposium on Close-Range Photogrammetry, *Proceedings* 1971.
4. Faig, W., and H. Moniwa, "Convergent Photos for Close-Range," *Photogrammetric Engineering*, 39:605-610, 1973.
5. Herron, R. E. "Close-Range Stereophotogrammetry—A Bridge Between Medicine and Photogrammetric Engineering," *Proceedings* of A.S.P. 1959 Convention.
6. Karara, H. M. "Stereometric Systems of High Precision," *Proceedings* International Symposium I.S.P. 1966.
7. Kenefick, J. F. "Ultra-Precise Analytical Stereotriangulation for Structural Measurements," A.S.P. Symposium on Close-Range Photogrammetry, *Proceedings* 1971.
8. Lippert, F. G. "The Three Dimensional Measurements of the Tibia Fracture Motion by Photogrammetry," *Clin. Orthopaedics*, 1974.
9. Lippert, F. G., M. Hussain, and S. A. Veress, "Measurement of Spatial Motion Using Close-Range Analytical Photogrammetric Principles," *Proceedings* A.S.P.-A.C.S.M. 1970.
10. Veress, S. A. *Adjustment Computation*, American Congress on Surveying and Mapping, 1974.
11. Veress, S. A., C. Y. Hou, and J. W. Prothero, "A Quantitative Study of Biological Form," *I.E.E.E., Trans. Biomed. Eng.* 17:106, 1970.
12. Veress, S. A. "The Use and Adoption of Conventional Stereoplotting Instruments for Bridging and Plotting of Super Wide Angle Photography," *The Canadian Surveyor*, Vol. 23: 359-376, 1969.